

High-precision tabletop microplotter for flexible on-demand material deposition in printed electronics and device functionalization F

Cite as: Rev. Sci. Instrum. **92**, 125104 (2021); <https://doi.org/10.1063/5.0061331>

Submitted: 25 June 2021 • Accepted: 19 October 2021 • Published Online: 07 December 2021

 Navid Hussain,  Mohammad Jan Nazami, Chunyan Ma, et al.

COLLECTIONS

F This paper was selected as Featured





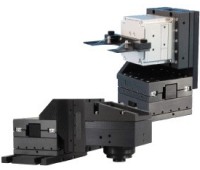
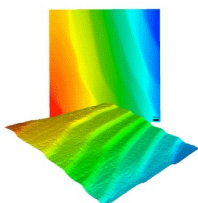
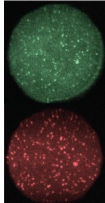
View Online



Export Citation



CrossMark

 <p>MCL MAD CITY LABS INC. www.madcitylabs.com</p>	<p>Nanopositioning Systems</p> 	<p>Modular Motion Control</p> 	<p>AFM and NSOM Instruments</p> 	<p>Single Molecule Microscopes</p> 
--	--	--	---	--

High-precision tabletop microplotter for flexible on-demand material deposition in printed electronics and device functionalization

Cite as: Rev. Sci. Instrum. 92, 125104 (2021); doi: 10.1063/5.0061331

Submitted: 25 June 2021 • Accepted: 19 October 2021 •

Published Online: 7 December 2021



View Online



Export Citation



CrossMark

Navid Hussain,¹  Mohammad Jan Nazami,^{1,2}  Chunyan Ma,² and Michael Hirtz^{1,a)} 

AFFILIATIONS

¹Institute of Nanotechnology (INT) and Karlsruhe Nano Micro Facility (KNMF), Karlsruhe Institute of Technology (KIT), Hermann-von-Helmholtz-Platz 1, 76344 Eggenstein-Leopoldshafen, Germany

²College of Electrical and Power Engineering, Taiyuan University of Technology, Taiyuan 030024, China

^{a)}Author to whom correspondence should be addressed: michael.hirtz@kit.edu

ABSTRACT

Microstructuring, in particular, the additive functionalization of surfaces with, e.g., conductive or bioactive materials plays a crucial role in many applications in sensing or printed electronics. Mostly, the lithography steps are made prior to assembling functionalized surfaces into the desired places of use within a bigger device as a microfluidic channel or an electronic casing. However, when this is not possible, most lithography techniques struggle with access to recessed or inclined/vertical surfaces for geometrical reasons. In particular, for “on-the-fly” printing aiming to add microstructures to already existing devices on demand and maybe even for one-time trials, e.g., in prototyping, a flexible “micropencil” allowing for direct write under direct manual control and on arbitrarily positioned surfaces would be highly desirable. Here, we present a highly flexible, micromanipulator-based setup for capillary printing of conductive and biomaterial ink formulations that can address a wide range of geometries as exemplified on vertical, recessed surfaces and stacked 3D scaffolds as models for hard to access surfaces. A wide range of feature sizes from tens to hundreds of micrometer can be obtained by the choice of capillary sizes and the on-demand *in situ* writing capabilities are demonstrated with completion of a circuit structure by gold line interconnects deposited with the setup.

Published under an exclusive license by AIP Publishing. <https://doi.org/10.1063/5.0061331>

I. INTRODUCTION

The past decade has seen the rapid development of printed devices, and fully printed small-sized nano-/micro-electro-mechanical systems (NEMS/MEMS) devices are continuously arising. These developments have heightened the need to develop direct printing technologies to make these devices at low cost and stop material waste. Along with this growth, direct printing techniques have also transformed from a fascinating scientific curiosity into a valuable, reliable, and commercially available technology with broad applications in scientific research fields such as materials sciences, printed electronics, and life science. Applications of printing systems include flexible thin-film transistors,^{1,2} organic light emitting diode (OLED) arrays and transistors,³ radio-frequency identification (RFID) and antennas,^{4,5} triboelectric nanogenerators,⁶ nanophotonic circuits,⁷ environmental sensors such as temperature sensors,⁸ tactile sensors, two-dimensional force

sensors,⁹ humidity sensors,¹⁰ pressure sensors,¹¹ biosensors and wearable sensors,^{12,13} chemosensors,¹⁴ and a variety of other life science applications, including biological spotting,^{15–17} patterning of live cells,¹⁸ and proteomics.^{19,20} All of these devices and applications need high precision of deposition in a particular area and shape.

A number of printing methods exist for the addition of features onto a given surface such as stencil lithography,^{3,4} molding, embossing, screen printing, shadow mask printing,^{8,9,12} roll to roll printing, direct writing or additive manufacturing such as inkjet printing,^{1,2,4,10,13,14} aerosol printing,¹¹ laser printing (ablation, selective sintering, or reactive chemical processes),^{17,19,21} electron beam and focused ion beam based printing,⁵ microcontact printing and polymer pen lithography,^{15,22} nanotransfer printing, electrospray deposition,²³ electrochemical printing,²⁴ and scanning probe lithography techniques (with different probe-surface interaction mechanism such as mechanical, thermal, chemical, dip-pen

nanolithography, oxidation, bias and magnetic).^{7,16,25–29} These techniques can be divided into contact and non-contact printing methods or conventional and non-conventional printing systems based on the printing method. Other than that, printing systems can also be roughly divided into two groups according to technologies: high technology and accessible technology. High technology and complex instrumentation-based printing setups such as commercially available inkjet printing systems are expensive; these printing systems cost a hundred thousand euros for a printer and are afflicted by high maintenance. The center of attention to the printing techniques has been mostly restricted to these commercially available high-technology inkjet printing systems. Therefore, it is time to develop a low-cost, reliable, easy to use, tabletop accessible technology that could be assembled and operated without additional training as a complementary option.

Besides these features, accessible technology printing should also serve more reliability and greater resolution competitive to high technology and complex machinery based printing setups. Multiple partially accessible technology-based laboratory printing setups have recently been reported.^{18,30–33}

Here, we present an affordable tabletop technique, which can deposit materials in places that are non-accessible with conventional printers. This setup can deposit materials in a controlled manner with microscale resolution, micrometer precision, and highest

flexibility in pattern. With this turnkey printing setup, users will instantly start their work and printing according to the application without much training and assistance. We have also shown printed conductive microarrays and lines of gold on glass and Kapton film flexible substrates. These microdots and line structures represent the microelectrodes, soldering application for bonding semiconductor chips and printable and flexible electronics. Additionally, as an example of biomaterial inks, we show printing of inks containing lipids (DOPC), proteins [bovine serum albumin (BSA)], and small bioactive molecules (biotin).

II. THE MICROPLOTTER

A. Printing setup design

The main design criteria of the setup [Fig. 1(a)] were to (a) provide fast and easy assembly and (b) enable superior accessibility with regard to non-flat or otherwise hard to access surfaces to functionalize. Therefore, instead of relying on a micropositioning sample stage or a fixed spotting probe hovering above the sample as the most common design in present scanning probe lithography (SPL) setups, a highly versatile micromanipulator mini-robot (miBot, Imina Technologies) was chosen as the core component in the setup. The miBots are highly precise, compact, and non-tethered micromanipulators that can freely move in x–y on a metal plate and comprise

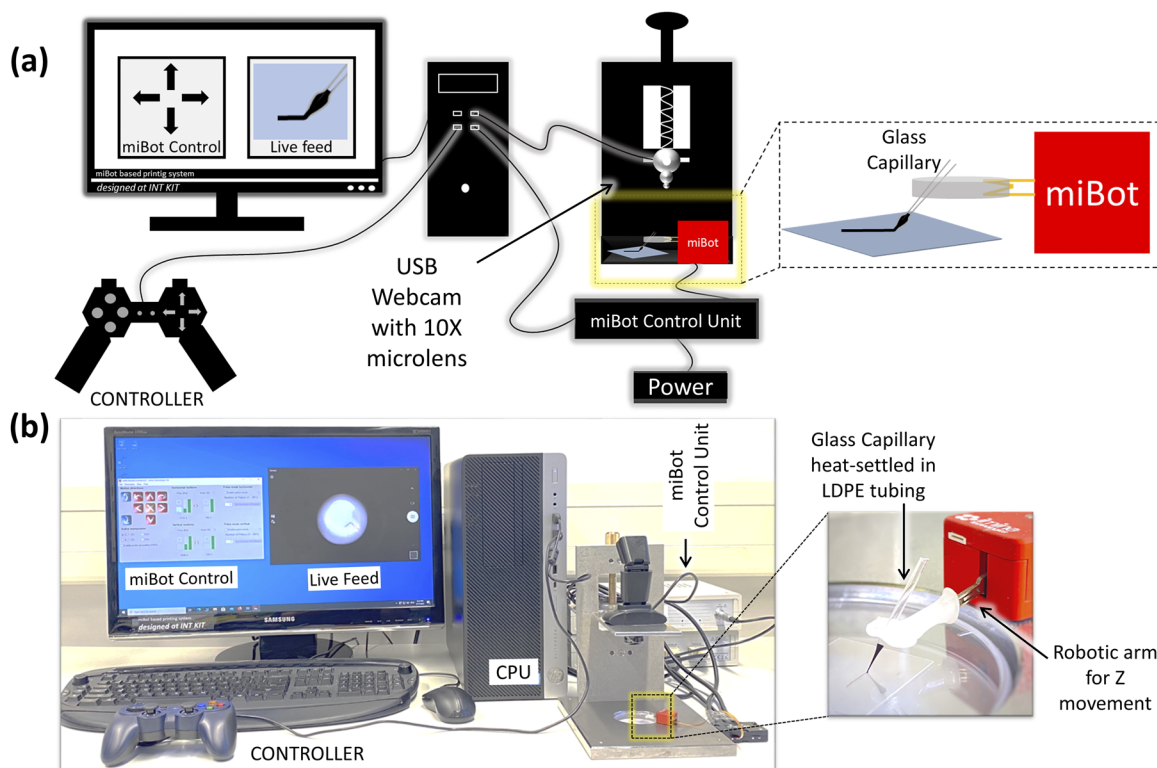


FIG. 1. The printing setup: (a) schematic representation and (b) photographs of the actual setup. The setup consists of a printing stage that carries a USB webcam above the sample area surrounded by a platform for the micromanipulator carrying a glass capillary on a robotic arm. The micromanipulator is connected to a personal computer (PC) over a control unit and can be controlled via a handhold controller while the positioning of the capillary over the sample can be monitored in the webcam.

an arm that can be raised or lowered, overall resulting in submicrometer positioning precision in 3D over several millimeters. These robots are frequently used in probe station setups for especially flexible contacting under challenging conditions³⁴ or for interactive micro- and nanomanipulation^{35,36} and nanomechanical studies.^{37,38} The platform for the micromanipulator is a steel frame (built in-house) that also holds a universal serial bus (USB) camera (Webcam 1080P, Wansview) with a microlens (10× mobile objective, Mpow), which supplants a microscope and allows real-time monitoring of the printing process. The camera is mounted on a height-adjustable head that allows for easy adjustment of the sample/camera distance over a wide range. This construction also allows free access to the sample from all sides and with ample headroom. There is an in-built groove available in the design to level the substrate; in the case of printing in-plane, this groove can be filled to provide a flat stage. On the other hand, while vertical printing, the 3D-printed substrate holder can be fixed in the groove to provide better accessibility to the surface.

The described platform allows a flexible rough positioning of the micromanipulator by simply setting it to a desired location by hand. From the starting position, the full high-precision workspace of $20 \times 20 \text{ mm}^2$ in X and Y and a Z movement of the arm of 42° can be accessed. Depending on the desired positioning precision, a maximum speed of 2.5 mm/s in x-y and 150 mrad/s in z movement can be achieved.^{39,40} To allow dispensing of ink by the micromanipulator, styluses were fabricated as follows: first, glass capillaries with various tip and taper sizes were prepared using a micropipette puller system (P-1000, Sutter Instruments) from glass capillaries of 100 mm length, with outer and inner diameters of 1.2 and 0.94 mm, respectively (GC120TF-10, without filament, Warner Instruments). Then, the prepared glass capillary was cut to a length of about 3 cm and heat-settled (using a heat gun, Steinel HG3000SLE) into a low-density polyethylene (LDPE) tubing (0.1/3 mm inner/outer diameter, Reichelt Chemietechnik). The 0.1 mm inner diameter of the tubing fits well to the micromanipulator arm and allows an easy mounting of the stylus. Importantly, the flexible LDPE tubing dampens vibrations during the printing process when the glass capillary contacts the sample.

All components used in the construction of the printing setup are tabulated in Table I.

The software used for control of the micromanipulator are the on-board miBot Remote Control software v 2.5.7 and the Preciso software suit v 1.6.4 (both by Imina Technologies). The mibots are usually operated in the stepping mode, where the speed and resolution are adjusted with the two parameters of frequency and amplitude of the driving signals. The frequency determines the movement speed of the mibots and the amplitude decides on the step size during the movement. The frequency and amplitude can be adjusted in the user interface and both parameters can be linked together so that when moving at high speed, the manipulator also utilizes bigger step sizes. Overall, this enables a wide range of movement speed and precision if needed: e.g., the maximal speed of movement for the manipulator is 2.5 mm/s in X and Y and 150 mrad/s in Z (arm movement) desirable for rough positioning on a sample, but then can be tuned down for highest precision (in principal) to 60 nm stepping in X and Y and 120 nm in Z in the stepping mode or even sub-nanometer in the scanning mode. Thus, the precision achievable in our setup is effectively limited by the optical resolution of the camera used and not by the manipulator. The movements of mibots are manually controlled with the help of the user interface or—making use in particular intuitive—by a handheld control pad.

B. Printing process

For a typical printing process (Fig. 2), first, a fresh glass capillary stylus is loaded on the robotic arm of the micromanipulator. Then, the manipulator is moved to the ink reservoir. Once the capillary from the stylus comes in contact with the ink reservoir, the ink is aspirated into the glass capillary nozzle tip via capillary force. After the capillary is filled, it is retracted from the inkwell and positioned to the pattern's desired starting point. Then, the inkwell and sample to write on are positioned right next to each other, which can be done by moving the micromanipulator by the software controls, but the inkwell can also be easily removed from the stage altogether and replaced with the desired sample. In this case, the micromanipulator can be roughly positioned with regard to the sample by hand after

TABLE I. Components of the printing setup.

Component	Type, supplier
System frame	Aluminum/steel, built in-house, STL file, https://www.doi.org/10.5445/IR/1000134042
Height adjustment for the webcam holder	Aluminum, built in-house, STL file, https://www.doi.org/10.5445/IR/1000134043
Substrate holder plate	Steel, built in-house, STL file, https://www.doi.org/10.5445/IR/1000134044
Webcam holder	Aluminum, built in-house, STL file, https://www.doi.org/10.5445/IR/1000134046
Sample holder (vertical printing example)	Thermoplastic, 3D-printed in-house, STL file, https://www.doi.org/10.5445/IR/1000134047
Scaffold structure (difficult access example)	Thermoplastic, 3D-printed in-house, STL file, https://www.doi.org/10.5445/IR/1000134048
Metallic sample holder (<i>in situ</i> curing example)	Metal filament, 3D-printed in-house, STL file, https://www.doi.org/10.5445/IR/1000134049
Camera	Webcam 1080P, Wansview
Lens	10× mobile objective, Mpow
Micromanipulator	miBot, Imina Technologies
Controller software	miBot remote control 2.5.7/Preciso Software Suite, Imina Technologies
Joypad	Gamepad F310, Logitech
Printing stylus	Glass capillary in LDPE mount, built in-house

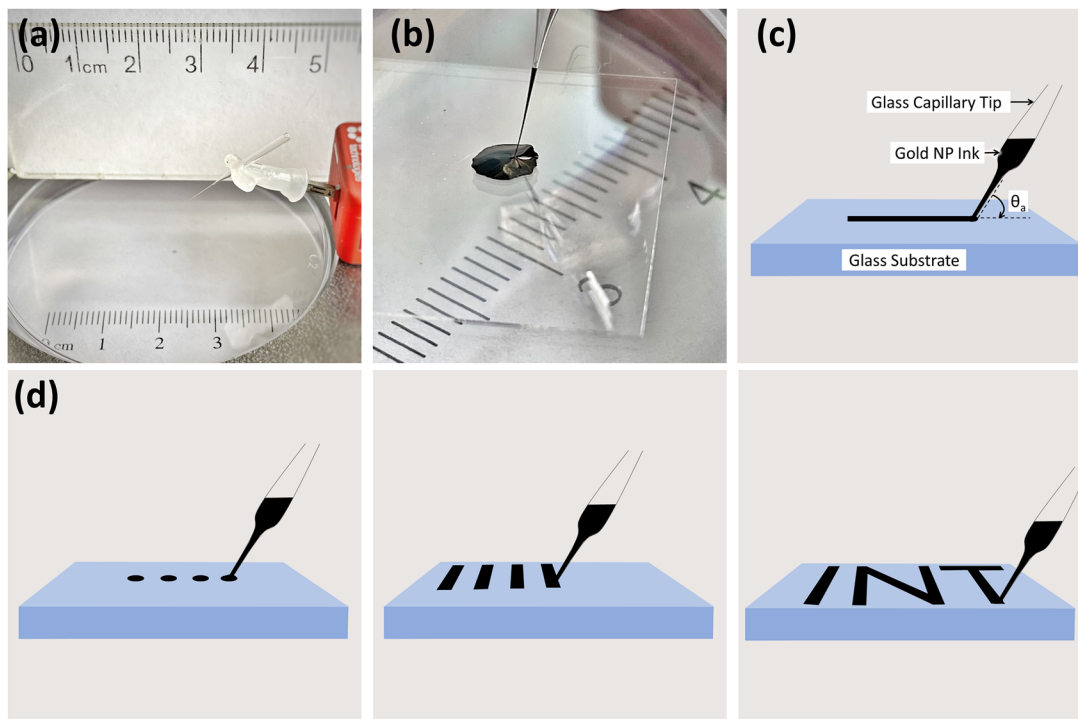


FIG. 2. The capillary stylus and the schematic of the printing process. (a) Photograph of the glass capillary stylus mounted on the micromanipulator. (b) Photograph of the capillary during the ink loading process in the “inkwell.” (c) Schematics of the geometry during the writing process. (d) Schemes of the writing process for dots, lines, and arbitrary curves.

the exchange (as it can be freely picked up from the stage and repositioned). Then, the glass capillary tip is brought near the substrate under software control to dispense a fluid spot on a surface. The USB camera with a $10\times$ objective microlens monitoring system displays the gentle physical contact between the stylus and the substrate. On contact between the substrate and the glass capillary tip, ink transfers from the glass capillary nozzle to the substrate. The duration of touch and the speed of movement play an integral part in the size of dots or the width of lines written. Once it touched the substrate, the micromanipulator unit is moved manually in a straight line or arbitrary curve according to the demand for the structure geometry, leaving behind the desired structure or pattern. Different shapes such as microarrays, lines, curves, and other structures can be printed on-the-fly (meaning on spontaneous decision of the user as needed). After the line or desired pattern is finished, the glass capillary stylus is retracted from the substrate, effectively separating the substrate and glass capillary tip and stopping the ink transfer. The process from mounting of the capillary to printing a pattern is very quick and implemented within 5 min for a simple dot or line pattern as shown in Sec. III.

C. Enhanced access to printing areas

By the open design and use of the robotic micromanipulator, the printing setup offers enhanced access to otherwise unreachable areas on a substrate and even allows for printing on vertical surfaces. For demonstration of this, glass substrates were fixed in a 3D-printed

frame (Fig. 3). Such a holder can also be used when printing on mainly flat substrates with lower laying areas or high aspect ratio trenches or troughs, which are often inaccessible by the conventional SPL printing setup by their respective geometry.

This “on-the-fly” writing capability combined with enhanced access makes the setup uniquely suited for difficult lithography tasks or one-time processes that can currently not be addressed well in conventional SPL setups. This will be demonstrated in Sec. III B.

III. RESULTS AND DISCUSSION

To demonstrate the capabilities of the printing setup, different types of ink and substrate materials as well as different substrate geometries were probed and results are characterized with relevance for different research fields such as printable electronics and bioactive surface functionalization.

A. Gold structures on glass and Kapton film

Conductive inks and flexible substrates are of high interest in the field of printable electronics. In our demonstration, a gold nanoparticle (NP) based ink (UTDAu25-IJ, UT Dots) was printed into dots and line structures in a printing process as described earlier. To obtain high-quality and conductive printed gold patterns, the glass substrates were annealed in a furnace (Nabertherm P330) to 250°C for 30 min after printing. Then, the patterns were inspected

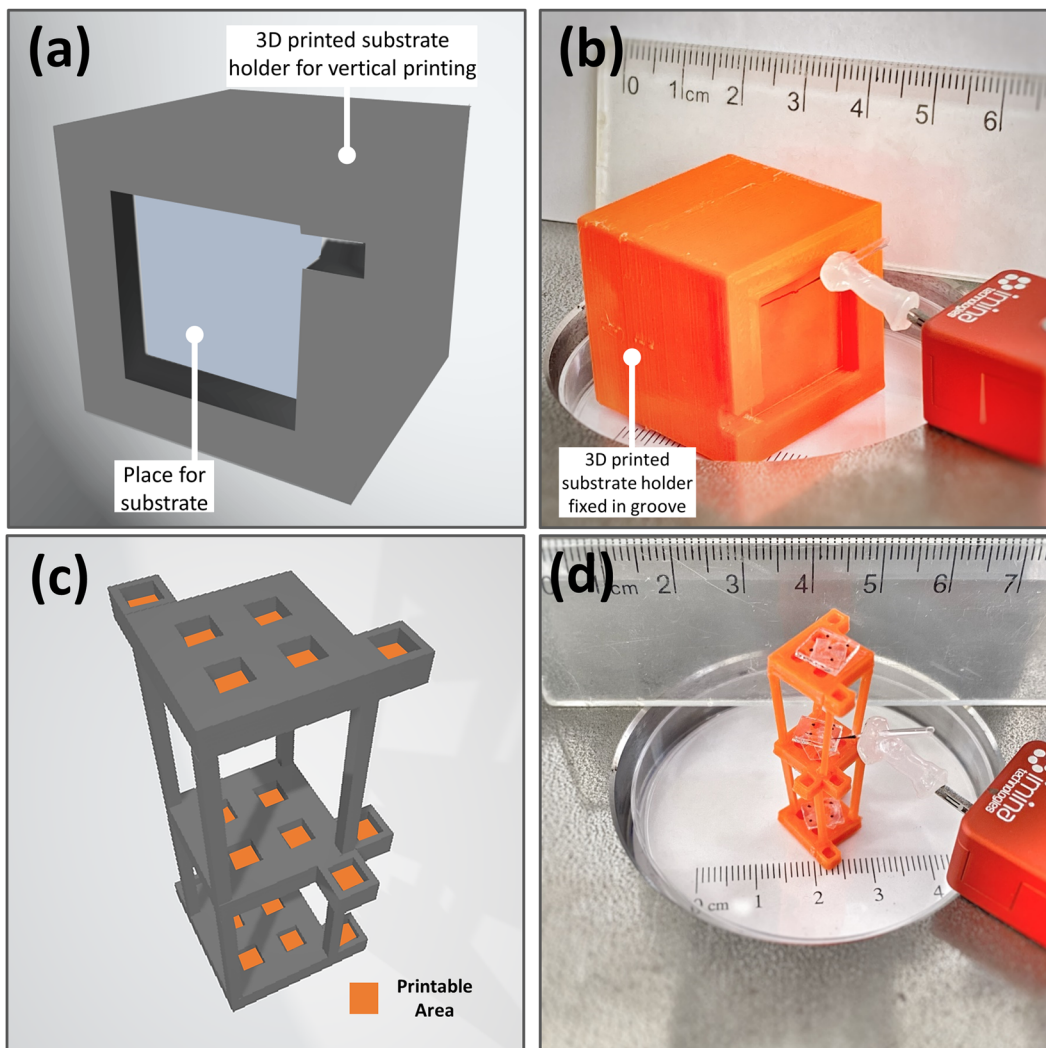


FIG. 3. Examples for “hard-to-access” surfaces. (a) Design scheme of a 3D-printed substrate holder for demonstration of vertical printing capabilities. (b) Photograph of the actual vertical printing setup with a micromanipulator and an ink-loaded capillary in place. (c) Design scheme of a complex holder structure to demonstrate printing capability at areas where a regular printer cannot reach. (d) Photograph of the actual multi-level printing setup again with a micromanipulator and an ink-loaded capillary in place.

via optical microscopy. Figure 4 displays a typical outcome of such gold ink printings on glass (glass coverslips, VWR) and Kapton foil (Kapton-HN, Dupont). All substrates were cleaned by subsequent sonication in chloroform, 2-propanol, and deionized water, and glass substrates were also rendered more hydrophilic by oxygen plasma (10 SCCM O_2 , 0.2 mbar, 100 W, 2 min, in a Diener ATTO B plasma cleaner) when necessary for printing outcome (see below).

The large working area of the micromanipulator and the easy manual control allows for free-hand writing of large structures as exemplified by the INT logo in Fig. 4(a). More careful control enables micropatterns of dots and lines. The obtained dot diameter and linewidth were also studied with regard to printing parameters such as dwell times and different tip sizes. Dwell time influence on the dot size was not significant [probed for 2, 5, and 10 s,

yielding an average of $(458.0 \pm 8.4) \mu\text{m}$]. The thickness of the dots was determined via tapping mode atomic force microscopy (Dimension Icon, Bruker) at a scratch through the middle of dot features yielding $(118 \pm 26) \text{nm}$. Varying tip sizes from 30 to 230 μm opening reveals feature sizes in the range of (23.6 ± 2.6) to $(458.0 \pm 8.4) \mu\text{m}$ diameter for dots and (15.9 ± 3.7) to $(389.4 \pm 19.9) \mu\text{m}$ for linewidths. Considering the simplicity of the overall setup, still sub-10 μm gap sizes between features could be achieved [Fig. 4(c)]. Pattern fidelity and definition is less good when printing on Kapton foil, as of the different spreading characteristics of inks on this substrate, but still features sizes around 200–500 μm are readily achieved [Figs. 4(e) and 4(f)]. This underlines the general point that the achieved resolution and pattern fidelity depend not only on the capillary size opening, but also even more crucial on the wetting behavior of the given ink/substrate combination. In particular, while

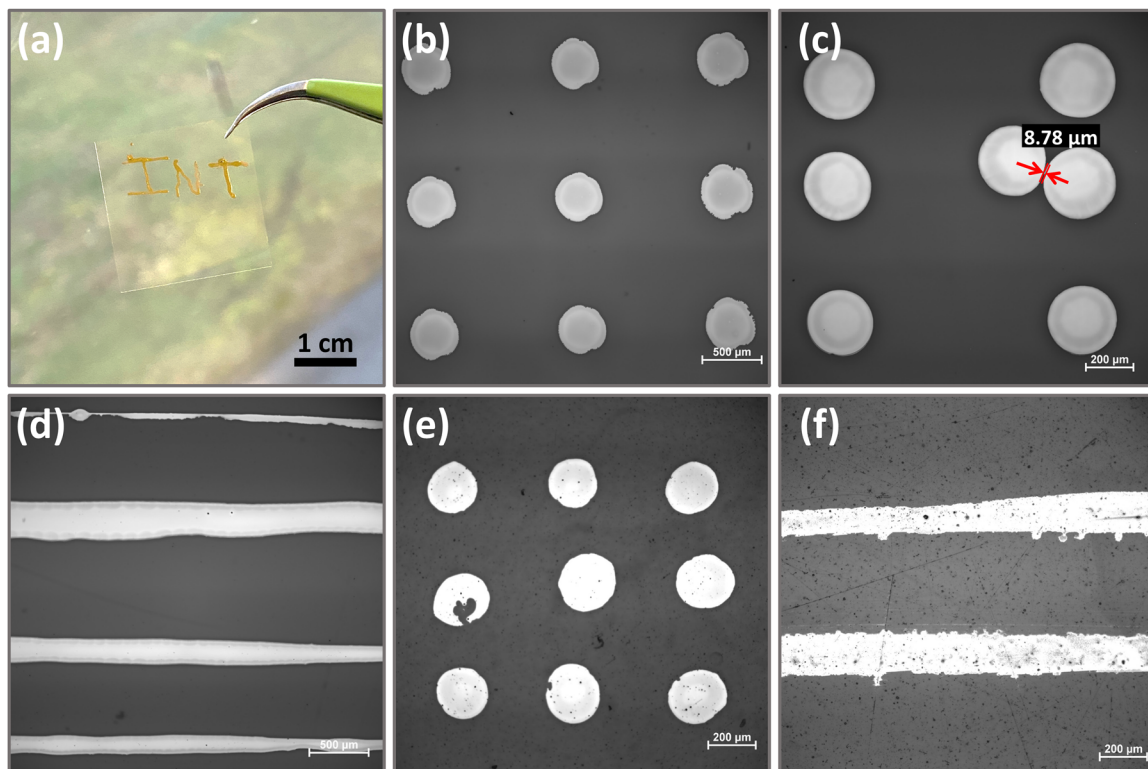


FIG. 4. Examples of gold patterns on glass and Kapton substrates: (a) photography of macroscopic letters “INT” printed on a glass substrate; bright-field microscopy images of (b) microdots on a glass substrate, (c) side-by-side printed dots with sub-10 μm gap distance on a glass substrate, (d) line structures of different width on a glass substrate, (e) microdots on a Kapton substrate, and (f) line structures on a Kapton substrate.

writing with smaller capillary tip sizes ($<50 \mu\text{m}$) and low contact angles, the gold ink was prone to adhere to the outside of the capillary rather than to the substrate, thus moving along with the capillary tip over the substrate, rather than depositing. Additionally, if the surface energy of the substrate is not sufficiently high, already written lines can break up into droplets by dewetting. These problems can be amended by adjusting writing speeds using wider capillaries and changing substrate wetting by plasma cleaning. Thus, overall, the printing process can be optimized with regard to and also by engineering the ink and substrate physico-chemical properties, e.g., the viscosity of ink, driving mode, wetting behavior, contact angle, drying effects, line spreading, and temperature conditions, similar to those in other spotting approaches or in inkjet printing.

B. Flexible on-demand interconnects for printed electronics

Having shown the applicability of the printing approach to Au-NP inks in Sec. III A, we now apply the microplotter to achieve functional electrical circuits. The enhanced accessibility provided by the setup enables flexible on-demand interconnects to be created *in situ* on already existing complex structures. To demonstrate this, a scaffold structure was 3D-printed in metal and equipped with a recessed glass substrate carrying a couple of (hand-drawn) macroscopic silver-epoxy-based electrodes connected to the

outside of the scaffold by Teflon-coated copper wires for connection of an LED and power supply. The scaffold holding the glass in a recessed cavity makes it arbitrarily inaccessible to standard printing methods to demonstrate the flexibility of the micromanipulator approach for *in situ* and on-demand printing of interconnects (Fig. 5).

While this prestructure device would not be readily accessible for conventional SPL methods without prior disassembly, now all functionalization steps can take place *in situ*. The needed wiring to close pre-existing circuit can simply be applied to the device on-demand by direct writing the Au-NP ink in the desired layout between the pre-existing silver-epoxy based electrodes. After curing of the device, the interconnects become conductive and the circuit is rendered functional with an assembly of LEDs and power supply [Fig. 5(b)].

C. Deposition of protein inks

Many applications in biomedical research and health care applications, in particular, diagnostics, utilize surface immobilized biomaterials, often in the form of arrays. Here, one class of biomaterials with special importance are proteins. These can act, e.g., as antigens to detect the presence of antibodies, or in the form of antibodies themselves to detect antigens from a bodily fluid such as blood for diagnostic purposes, or can act as external stimuli, e.g.,

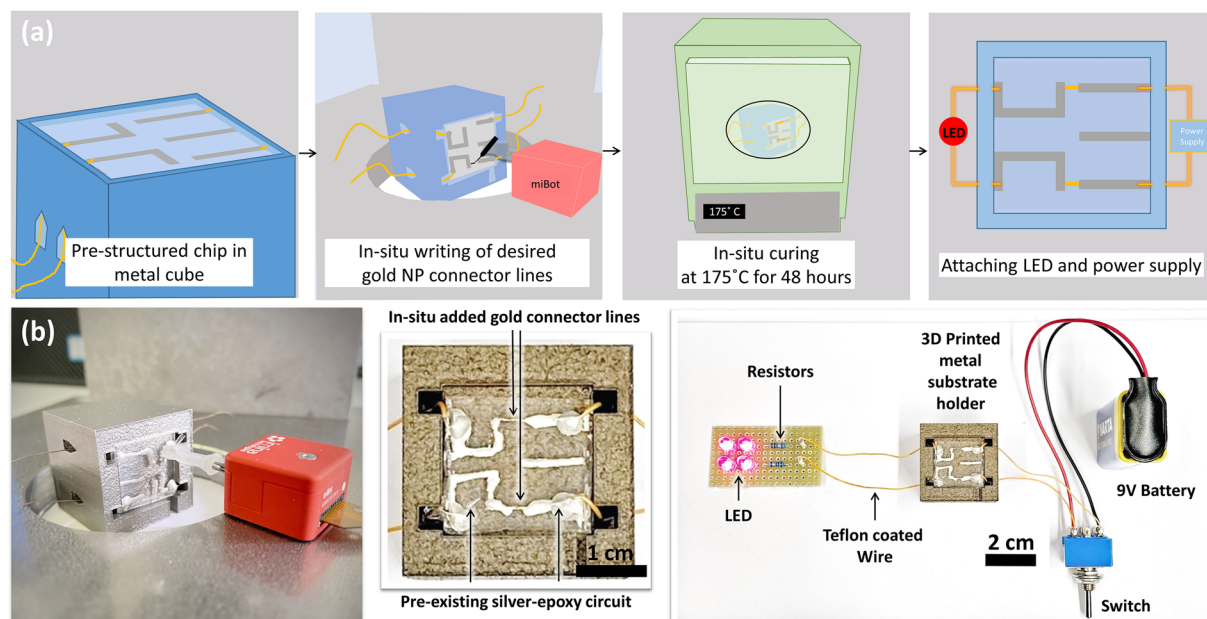


FIG. 5. *In situ* and on-demand writing of connectors. (a) Schematic workflow: a glass chip with pre-structured (hand-drawn) silver-epoxy paste based electrodes recessed into a metal cube is used as a model device. The microplotter setup is then used to close the circuit with Au-NP connector lines written between the desired electrodes. The device is then cured in a furnace and LED and the power supply can be connected to demonstrate the function of the created circuit. (b) Photographs of an actual writing process and a typical result showing the fine gold connector lines obtained by the microplotter. After curing and assembly of the LED and power supply, the functionality of the circuit is demonstrated.

modifying cell adhesion or activation in biomedical experiments. In particular, while prototyping lab-on-chip devices, a flexible on-demand functionalization of surfaces within bigger structures such as microfluidic channels or wells (which can be hard to reach with conventional approaches for geometrical reasons) is searched for by researchers. Additionally, direct deposition of a small volume of an

analyte sample itself to a desired place within such a chip structure can be desired for testing purposes. Therefore, to demonstrate also the printing of biomaterial inks with the microplotter setup, we deposited inks containing fluorescence labels and different biological materials as lipids, proteins, or small bioactive molecules (details on inks are shown in Table II).

TABLE II. Ink formulations.

Ink description	Ink 1	Ink 2	Ink 3
Component A (biomaterial)	1,2-dioleoyl-sn-glycero-3-phosphocholine (DOPC) [supplied by Avanti Polar Lipids (USA)], concentration: 20 mg/ml in ethanol	Bovine serum albumin (BSA) (supplied by Invitrogen, Thermo Fisher Scientific), concentration: 50 mg/ml in water	Protein A-biotin from staphylococcus aureus (supplied by Sigma-Aldrich), concentration: 2 mg/ml in phosphate buffered saline (PBS)
Component B (avoiding ink drying)	Glycerol (supplied by Sigma-Aldrich)		
Component C (fluorescent label)	Rhodamine 6G (supplied by Sigma-Aldrich), concentration: 1 mg/ml in water	Fluorescein isothiocyanate (FITC)-PEG (PG2-FCTH-1k, supplied by NANOCS), concentration: 1 mg/ml in water	Alexa fluor 647 azide, triethylammonium salt (A10277, Life Technologies, Thermo Fisher), concentration: 0.5 mg/ml in DMSO
Volumetric ratio (%) (A:B:C)	60:35:5	60:35:5	60:30:10

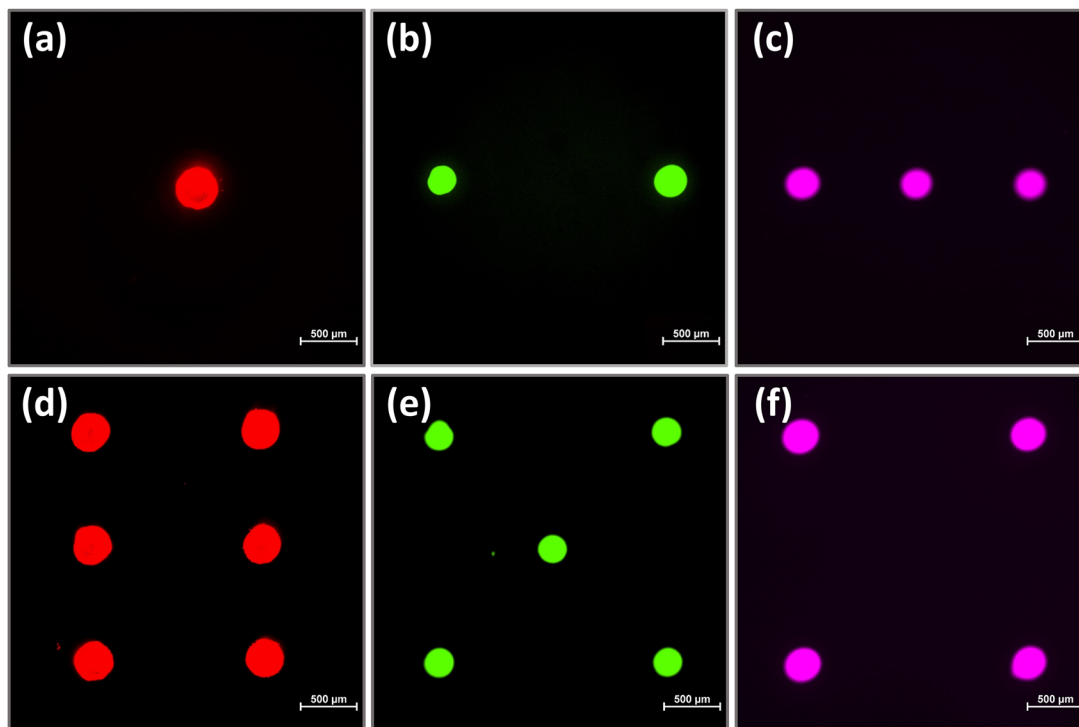


FIG. 6. Fluorescence microscopy images of the deposited bioink pattern. Different spot configurations were plotted with ink 1 (a) and (d), ink 2 (b) and (e), and ink 3 (c) and (f). Red channel: Texas Red filter set (Y-2E/C, Nikon, Ex.: 540–580 nm, Em.: 600–660 nm), green channel: FITC filter set (B-2E/C, Nikon, Ex.: 465–495 nm, Em.: 515–555 nm), and purple channel: Cy5 filter set (AHF F41-008, Nikon, Ex.: 590–650 nm, Em.: 662–738 nm).

After loading the inks into the capillary as described in Sec. II B, different spot patterns were written with the respective inks on glass surfaces. Figure 6 shows fluorescence microscopy images (obtained on an Eclipse 80i, equipped with a DS-Qi2 camera and C-HGFIE Intensilight, Nikon) of the resulting bioink dot configurations. Dots with diameters of (357.9 ± 16.0) , (257.0 ± 13.6) , and (291.5 ± 13.6) μm were achieved for ink 1, ink 2, and ink 3, respectively.

IV. CONCLUSION AND FUTURE PERSPECTIVES

We designed and implemented an open-source microprinting system that allows for flexible and highly accessible on-demand microplotting on samples and devices otherwise hard to address with conventional spotting methodologies. The setup provides a straightforward installation, configuration, and hassle-free operation without special training and offers competitive resolution and precision. It provides a “microfountain pen” to the user enabling flexibility in patterning with regard to the geometry and process flexibility, not unlike macroscopic handwriting. While microhandwriting, e.g., on rice grains is generally just seen as curiosity for peculiar records,⁴¹ with only the most skilled humans achieving (near)-microscale patterning by hand after years of practice, this setup can be used intuitively as a direct access to the microrealm for everyone. We demonstrated the use of the system in model applications for printable electronics and bioactive device functionalization,

exemplifying the broad material compatibility and flexibility of the substrate. It can provide printing of various aqueous solutions and solvent-based liquids in a wide viscosity range. Based on the presented ink systems, it would be straightforward to print other materials such as suspensions of graphene or carbon nanotubes, conductive polymers, nano/microparticle mixtures, DNA, and protein inks in microscale spots, lines, and different shapes with ease of accessibility and flexibility. The ink/substrate range could be broadened even further by integration of an active ink delivery system (e.g., syringe pump or microfluidic controller) to the glass capillary stylus, omitting the capillary force relying ink transfer mode presented here. Further control in printing could also be achieved by inclusion of the setup within a humidity chamber if desired for certain types of inks or substrates. In general, it should be noted that the achievable minimal feature size is highly dependent on the interaction of the ink and substrate, i.e., in particular, the surface tension of ink and the surface energy of the substrate. Combining the setup with more powerful optics would also allow us to fully leverage the micromanipulator robots positioning precision enabling not only functionalization of hard to reach surfaces but also pre-existing microstructures itself, e.g., for 3D-printed complex microcylinder structures in cell experiments.⁴² It would also be conceivable to add other stylus designs allowing for multi-ink deposition, e.g., by parallel arrays of miniaturized capillaries, or using other printing principles as, e.g., in arrays of microchannel cantilevers⁴³ or miniaturized polymer pen lithography such as stamps⁴⁴ (thus all of these would need conformal

leveling, complicating manual control). In summary, the setup offers high accessibility and ease-of-use for flexible on-demand functionalization ranging from the micro- to mm scale, a broad flexibility in ink and substrate materials, all intuitively controlled by joystick, making this tool a great “direct-write pencil” for researchers to quickly achieve *in situ* functionalization of devices.

ACKNOWLEDGMENTS

This work was partly carried out with the support of the Karlsruhe Nano Micro Facility (KNMF, www.knmf.kit.edu), a Helmholtz Research Infrastructure at the Karlsruhe Institute of Technology (KIT, www.kit.edu).

AUTHOR DECLARATIONS

Conflict of Interest

The authors have no conflicts to disclose.

DATA AVAILABILITY

The STL files of the microplotter setup are openly available in the KITopen repository at <https://www.bibliothek.kit.edu/kitopen.php> under the DOIs tabulated in Table I. The data that support the findings of this study are available from the corresponding author upon reasonable request.

REFERENCES

- 1 K. Fukuda, Y. Takeda, Y. Yoshimura, R. Shiwaku, L. T. Tran, T. Sekine, M. Mizukami, D. Kumaki, and S. Tokito, *Nat. Commun.* **5**, 4147 (2014).
- 2 T. Minamiki, T. Minami, Y.-P. Chen, T. Mano, Y. Takeda, K. Fukuda, and S. Tokito, *Commun. Mater.* **2**, 8 (2021).
- 3 J. Liu, J. Wang, Z. Zhang, F. Molina-Lopez, G.-J. N. Wang, B. C. Schroeder, X. Yan, Y. Zeng, O. Zhao, H. Tran, T. Lei, Y. Lu, Y.-X. Wang, J. B.-H. Tok, R. Dauskardt, J. W. Chung, Y. Yun, and Z. Bao, *Nat. Commun.* **11**, 3362 (2020).
- 4 C. L. Baumbauer, M. G. Anderson, J. Ting, A. Sreekumar, J. M. Rabaey, A. C. Arias, and A. Thielens, *Sci. Rep.* **10**, 16543 (2020).
- 5 M. Horák, K. Bukvišová, V. Švarc, J. Jaskowicz, V. Krápek, and T. Šikola, *Sci. Rep.* **8**, 9640 (2018).
- 6 L.-B. Huang, J.-C. Han, S. Chen, Z. Sun, X. Dai, P. Ge, C.-H. Zhao, Q.-Q. Zheng, F.-C. Sun, and J. Hao, *Nano Energy* **84**, 105873 (2021).
- 7 P. Rath, M. Hirtz, G. Lewes-Malandrakis, D. Brink, C. Nebel, and W. H. P. Pernice, *Adv. Opt. Mater.* **3**, 328 (2015).
- 8 Y.-F. Wang, T. Sekine, Y. Takeda, K. Yokosawa, H. Matsui, D. Kumaki, T. Shiba, T. Nishikawa, and S. Tokito, *Sci. Rep.* **10**, 2467 (2020).
- 9 S. Harada, K. Kanao, Y. Yamamoto, T. Arie, S. Akita, and K. Takei, *ACS Nano* **8**, 12851 (2014).
- 10 P. He, J. R. Brent, H. Ding, J. Yang, D. J. Lewis, P. O'Brien, and B. Derby, *Nanoscale* **10**, 5599 (2018).
- 11 J. B. Andrews, J. A. Cardenas, C. J. Lim, S. G. Noyce, J. Mullett, and A. D. Franklin, *IEEE Sens. J.* **18**, 7875 (2018).
- 12 T. Sekine, R. Sugano, T. Tashiro, J. Sato, Y. Takeda, H. Matsui, D. Kumaki, F. Domingues Dos Santos, A. Miyabo, and S. Tokito, *Sci. Rep.* **8**, 4442 (2018).
- 13 E. Bihar, S. Wustoni, A. M. Pappa, K. N. Salama, D. Baran, and S. Inal, *npj Flexible Electron.* **2**, 30 (2018).
- 14 E. Song, R. P. Tortorich, T. H. da Costa, and J.-W. Choi, *Microelectron. Eng.* **145**, 143 (2015).
- 15 A. Angelin, U. Bog, R. Kumar, C. M. Niemeyer, and M. Hirtz, *Polymers* **11**, 891 (2019).
- 16 M. Hirtz, A. Oikonomou, T. Georgiou, H. Fuchs, and A. Vijayaraghavan, *Nat. Commun.* **4**, 2591 (2013).
- 17 M. Colina, P. Serra, J. M. Fernández-Pradas, L. Sevilla, and J. L. Morenza, *Biosens. Bioelectron.* **20**, 1638 (2005).
- 18 A. Hacohen, H. R. Jessel, A. Richter-Levin, and O. Shefi, *Micromachines* **11**, 505 (2020).
- 19 J. A. Barron, H. D. Young, D. D. Dlott, M. M. Darfler, D. B. Krizman, and B. R. Ringeisen, *Proteomics* **5**, 4138 (2005).
- 20 H. Wagner, Y. Li, M. Hirtz, L. Chi, H. Fuchs, and A. Studer, *Soft Matter* **7**, 9854 (2011).
- 21 J. Bian, L. Zhou, X. Wan, C. Zhu, B. Yang, and Y. Huang, *Adv. Electron. Mater.* **5**, 1800900 (2019).
- 22 I.-N. Lee, J. Hosford, S. Wang, J. A. Hunt, J. M. Curran, W. P. Heath, and L. S. Wong, *J. Visualized Exp.* **136**, e56967 (2018).
- 23 V. N. Morozov and T. Y. Morozova, *Anal. Chem.* **71**, 3110 (1999).
- 24 X. Chen, X. Liu, M. Ouyang, J. Chen, O. Taiwo, Y. Xia, P. R. N. Childs, N. P. Brandon, and B. Wu, *Sci. Rep.* **9**, 3973 (2019).
- 25 H. Wagner, M. K. Brinks, M. Hirtz, A. Schäfer, L. Chi, and A. Studer, *Chem. - Eur. J.* **17**, 9107 (2011).
- 26 G. Liu, M. Hirtz, H. Fuchs, and Z. Zheng, *Small* **15**, 1900564 (2019).
- 27 R. D. Piner, J. Zhu, F. Xu, S. Hong, and C. A. Mirkin, *Science* **283**, 661 (1999).
- 28 R. Garcia, A. W. Knoll, and E. Riedo, *Nat. Nanotechnol.* **9**, 577 (2014).
- 29 S. A. M. Carnally and L. S. Wong, *Nanoscale* **6**, 4998 (2014).
- 30 T. H. da Costa and J.-W. Choi, *Micro Nano Syst. Lett.* **8**, 2 (2020).
- 31 B. Y. Ahn, E. B. Duoss, M. J. Motala, X. Guo, S.-I. Park, Y. Xiong, J. Yoon, R. G. Nuzzo, J. A. Rogers, and J. A. Lewis, *Science* **323**, 1590 (2009).
- 32 J. W. Boley, E. L. White, G. T.-C. Chiu, and R. K. Kramer, *Adv. Funct. Mater.* **24**, 3501 (2014).
- 33 G. M. Gratson, M. Xu, and J. A. Lewis, *Nature* **428**, 386 (2004).
- 34 W. Courbat and J. Jatzkowski, *Electron. Device Failure Anal.* **21**, 22 (2019); available at <https://static.asminternational.org/EDFA/201911/28/>.
- 35 W. Geng, S. Kostcheev, C. Sartet, V. Sallet, M. Molinari, O. Simonetti, G. Léronnel, L. Giraudet, and C. Couteau, *Phys. Status Solidi C* **10**, 1292 (2013).
- 36 M. Power and G.-Z. Yang, in *2015 IEEE/RSJ International Conference on Intelligent Robots and Systems (IEEE)*, pp. 790–797.
- 37 E. F. Arkan, D. Sacchetto, I. Yildiz, Y. Leblebici, and B. E. Alaca, *J. Micromech. Microeng.* **21**, 125018 (2011).
- 38 D. Thuau, C. Ayela, P. Poulin, and I. Dufour, *Sens. Actuators, A* **209**, 161 (2014).
- 39 See <https://www.eden-instruments.com/en/in-operando-eq> for Eden Instruments.
- 40 M. Hunstig, *Actuators* **6**, 7 (2017).
- 41 E. g. Surendra Kumar, Apharya was reported to being registered in the Guinness Book of world records 7 times, among others for writing 1749 characters on a single grain of rice.
- 42 J. Harberts, C. Fendler, J. Teuber, M. Siegmund, A. Silva, N. Rieck, M. Wolpert, R. Zierold, and R. H. Blick, *ACS Nano* **14**, 13091 (2020).
- 43 J. Xu, M. Lynch, S. Nettikadan, C. Mosher, S. Vegasandra, and E. Henderson, *Sens. Actuators, B* **113**, 1034 (2006).
- 44 F. Brinkmann, M. Hirtz, A. M. Greiner, M. Weschenfelder, B. Waterkotte, M. Bastmeyer, and H. Fuchs, *Small* **9**, 3265 (2013).